Climate Projections Used for the Assessment of the Western United States

By Anne Wein, Todd J. Hawbaker, Richard A. Champion, Jamie L. Ratliff, Benjamin M. Sleeter, and Zhiliang Zhu

Chapter 7 of

Baseline and Projected Future Carbon Storage and Greenhouse-Gas Fluxes in Ecosystems of the Western United States

Edited by Zhiliang Zhu and Bradley C. Reed

Professional Paper 1797

U.S. Department of the Interior
U.S. Geological Survey

U.S. Department of the Interior
KEN SALAZAR, Secretary

U.S. Geological Survey
Marcia K. McNutt, Director

U.S. Geological Survey, Reston, Virginia: 2012

For more information on the USGS—the Federal source for science about the Earth, its natural and living resources, natural hazards, and the environment, visit http://www.usgs.gov or call 1–888–ASK–USGS.

For an overview of USGS information products, including maps, imagery, and publications, visit http://www.usgs.gov/pubprod

To order this and other USGS information products, visit http://store.usgs.gov

Any use of trade, product, or firm names is for descriptive purposes only and does not imply endorsement by the U.S. Government.

Although this report is in the public domain, permission must be secured from the individual copyright owners to reproduce any copyrighted materials contained within this report.

Suggested citation:
Wein, Anne, Hawbaker, T.J., Champion, R.A., Ratliff, J.L., Sleeter, B.M., and Zhu, Zhiliang, 2012, Introduction to scope, methodology, and ecosystems of the assessment, chap. 7 *of* Zhu, Zhiliang, and Reed, B.C., eds., Climate projections used for the assessment of the Western United States: U.S. Geological Survey Professional Paper 1797, 10 p. (Also available at http://pubs.usgs/gov/pp/1797.)

Contents

7.1. Highlights....1
7.2. Introduction....1
7.3. Climate Patterns....4
7.3.1. Baseline Climate Patterns of the Western United States....4
7.3.2. Projected Climate Patterns of the Western United States....4
7.4. Summary and Discussion of Caveats Using the Climate Data....9

Figures

7.1. Maps showing the baseline (1970–1999) seasonal mean daily temperature (in degrees Celsius, °C) and total precipitation (in centimeters) by season 2
7.2. Chart showing the baseline summaries of mean daily temperature (in degrees Celsius, °C) and total precipitation (in centimeters) by season and grouped by both level II and level III ecoregions 3
7.3. Maps showing the projected changes in mean daily temperature (in degrees Celsius, °C) and total precipitation (in centimeters) by season, calculated using the difference in mean values from 2040 to 2069 and from 1970 to 1999 5
7.4. Chart showing summaries of the projected seasonal changes in mean daily temperature (in degrees Celsius, °C) and total precipitation (in centimeters) by season and grouped by both level II and III ecoregions for all general circulation models and scenarios 6

Tables

7.1. Projected changes in precipitation patterns derived from averaging the results from all the scenarios and general circulation models 8

This page intentionally blank

Chapter 7. Climate Projections Used for the Assessment of the Western United States

By Anne Wein[1], Todd J. Hawbaker[2], Richard A. Champion[1], Jamie L. Ratliff[1], Benjamin M. Sleeter[1], and Zhiliang Zhu[3]

7.1. Highlights

- Models of projected climate change were used in this assessment to further interpret the effects of climate change on the potential for carbon sequestration and greenhouse-gas (GHG) emissions in terrestrial ecosystems in the ecoregions of the Western United States. Climate-change data were used to support two modeling exercises: future potential wildland-fire emissions (chapter 8 of this report) and future potential carbon storage and sequestration (chapter 9 of this report).
- Climate-change data were represented in three general circulation models (GCMs) for each of three scenarios (A1B, A2, B1). The models of wildland fires and the biogeochemical modeling of carbon and GHGs used different sources of downscaling for the same GCMs because of the tasks' unique requirements. The projected patterns of precipitation differed between the two sources, particularly in mountainous areas.
- The models indicated a projected seasonal increase in mean temperature throughout the Western United States. Warming was projected to be most prevalent in summer and fall and in the eastern part of the Western United States.
- The projected warming was greater in scenarios A1B and A2; the MIROC 3.2-medres model projected the most warming and the CSIRO–Mk3.0 model projected the least. The projected increases in seasonal temperature extremes (minimums and maximums) generally followed patterns of projected increases in mean temperature.
- The projected precipitation patterns were highly variable among the GCMs, scenarios, seasons, and within the level II ecoregions, which necessitated the analyses of variabilities within each ecoregion.
- The variability in temperature and precipitation changes of the GCMs made the ranges of climate change for each scenario less distinct.

7.2. Introduction

Climate-change projections are required for modeling future potential ecosystem properties and processes. This chapter characterizes the baseline climate data and the projected climate-change data from general circulation models (GCMs); these data were used in this assessment for the wildland-fire-emission modeling discussed in chapter 8 and for the terrestrial ecosystem carbon-storage and GHG-flux modeling discussed in chapter 9. The relation between this chapter and other chapters of this report is shown in figure 1.2 of chapter 1 of this report, where climate data is featured in the "input data" and "climate projections" boxes of the diagram.

The term "climate change" refers to the changes in daily and weekly weather over months, seasons, centuries, and millennia. The climate affects the carbon cycle in terrestrial and aquatic systems through biogeochemical processes and natural disturbances (such as wildland fires), and also influences where land-use and land-cover (LULC) changes occur. This assessment sought to answer two questions related to the effects of climate change on carbon sequestration and GHG fluxes: (1) What are the projected potential changes to the critical climate variables within the ecoregions of the Western United States, and (2) What are the uncertainties for the climate-change projections in each of the ecoregions?

The climate-change data described here, along with the projected LULC scenarios (chapter 6) were aligned with the Intergovernmental Panel on Climate Change's Special Report on Emission Scenarios (IPCC–SRES; Nakicenovic and others, 2000). Although multiple scenarios (A1B, A2, and B1) provided the emission projections, the assessment used outputs from the GCMs, which were forced by the scenarios to capture the uncertainties of the analyses. The three GCMs used in this study are The Third Generation Coupled Global Climate Model of the Canadian Centre for Climate Modelling and Analysis (CCCma CGCM 3.1), Australia's Commonwealth Scientific and Industrial Research Organisation Mark 3.0 (CSIRO–Mk3.0) model, and the Model for Interdisciplinary Research on Climate version 3.2, medium resolution (MIROC 3.2-medres). The selection of GCMs represents a range of projected climate change that was constrained by the availability of suitably downscaled versions and resources to simulate multiple effects of climate change.

[1]U.S. Geological Survey, Menlo Park, Calif.

[2]U.S. Geological Survey, Denver, Colo.

[3]U.S. Geological Survey, Reston, Va.

The GCMs are mathematical representations of atmospheric, oceanic, cryospheric, and land-surface processes that express how those processes interact and respond to changes in GHG concentrations (Randall and others, 2007; U.S. Climate Change Science Program (CCSP), 2008). The GCMs subdivide the world into volumetric pixels (voxels) representing the layers of the atmosphere, land, and ocean at regularly spaced locations. The GCM outputs may include hourly, daily, and monthly estimates of temperature, precipitation, air pressure, wind, cloud cover, soil moisture, snow, humidity, or short- and long-wave fluxes of solar radiation. According to McAvaney and others (2001), projected surface-air temperatures generally have less uncertainty than projected precipitation, whereas projected cloud cover and humidity have the greatest uncertainty. Each GCM made different assumptions about global energy budgets; therefore, no single GCM projection was considered to be valid on its own and multiple models complement each other (Pierce and others, 2009). The components of this assessment that relied on GCM outputs incorporated data from multiple GCMs to help characterize uncertainties in climate projections.

The GCM outputs generally were produced at a coarse spatial resolution on the order of 1° to 3°, and spatial downscaling was performed to produce the resolution required for regional analyses. Fowler and others (2007) observed that, in general, downscaled temperature variables were more consistent with the original data than downscaled precipitation variables; downscaled winter climate variables were more consistent with the original data than downscaled summer climate variables; and downscaled wetter climate variables were more consistent with the original data than downscaled drier climate variables. These temperature and precipitation observations were not confirmed in a separate study for the Western United States (Pierce and others, 2009). Temperature and precipitation were the most common variables used in this assessment when the influence of climate change on carbon cycling was simulated. Other climate-related variables, such as humidity, were then derived from temperature and precipitation. Therefore, the discussion of potential climate change focuses on temperature and precipitation variables.

Climate and weather input data were required in order to model both wildland fires (chapters 3 and 8) and biogeochemical processes of carbon and GHG fluxes (chapters 5 and 9); however, two sources of downscaled climate and weather data were used for the same GCMs because of the unique requirements of the respective models.

The wildland-fire analyses (chapters 3 and 8) required daily weather data, including temperature, precipitation, relative humidity, and wind speeds for both the baseline and future time periods. The daily weather data were originally measured at weather stations, but were interpolated to 1/8° spatial resolution (approximately 12 km) for the conterminous United States (Maurer and others, 2002). These data span the years 1950 to 2010 and include minimum and maximum daily temperature and daily precipitation. The afternoon wind speeds and directions were taken from the 1/3° (approximately 32-km resolution) North American Regional Reanalysis data (Mesinger and others, 2006) and were joined to the daily temperature and precipitation data assembled by Maurer and others (2002). To model projected future wildland fires and emissions, the data from the three GCMs and the three climate-change scenarios were corrected for biases and downscaled to the baseline weather data (Maurer and others, 2002, 2007). Figures 7.1 and 7.2 show the baseline (1970–1999) mean daily temperature (in degrees Celsius, °C) and total precipitation (in centimeters) by season in both map and graph formats, which are based on data from Maurer and others (2002).

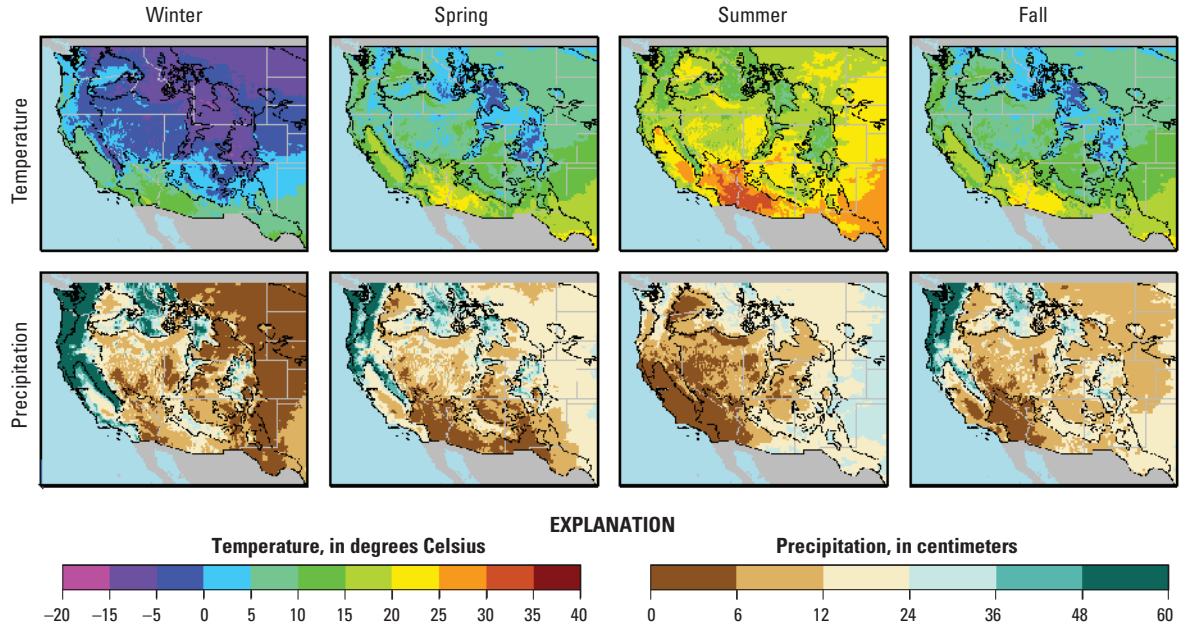

Figure 7.1. Maps showing the baseline (1970–1999) seasonal mean daily temperature (in degrees Celsius, °C) and total precipitation (in centimeters) by season. Data were from Maurer and others (2002). Winter included December, January, and February; spring included March, April, and May; summer included June, July, and August; and fall included September, October, and November.

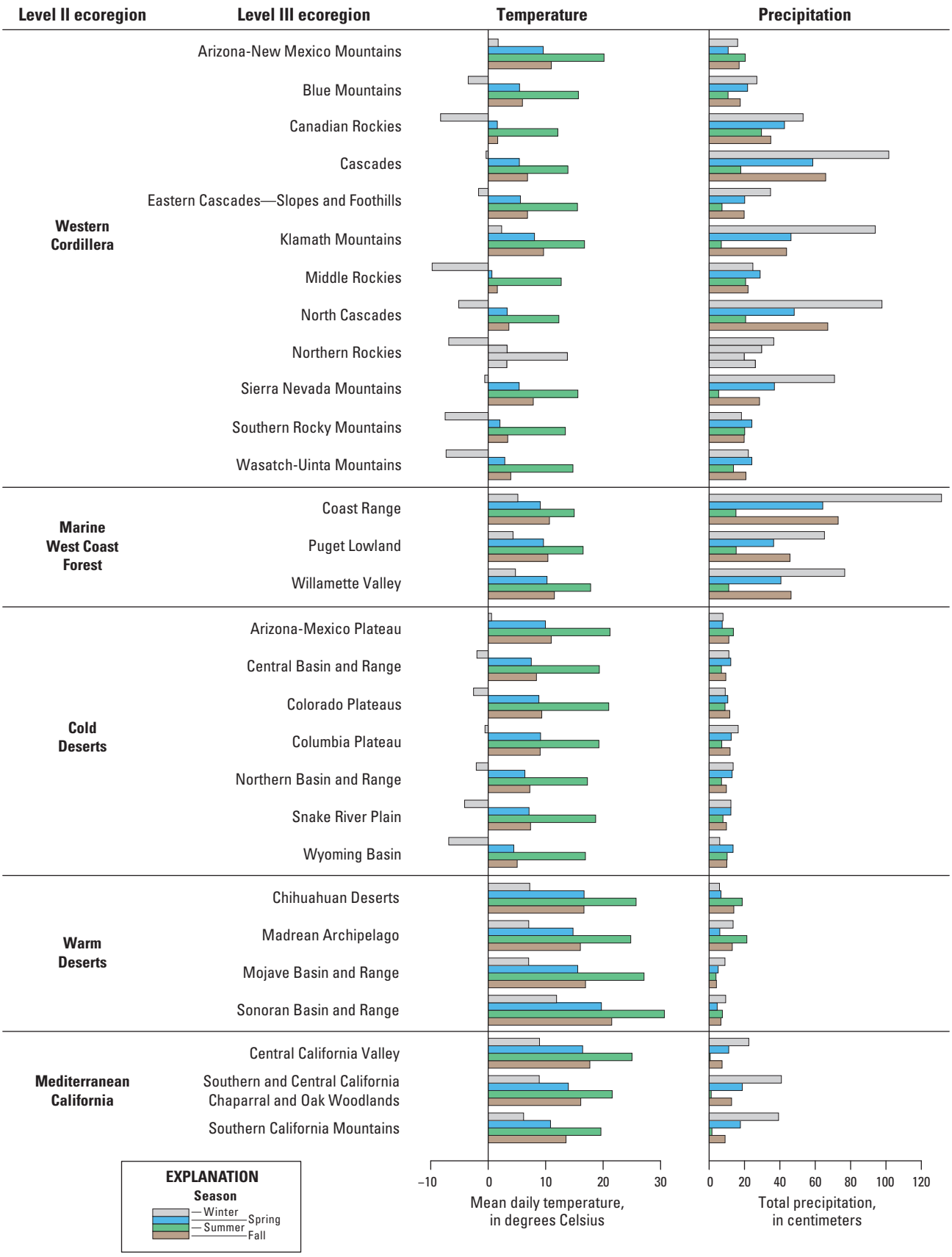

Figure 7.2. Chart showing the baseline summaries of mean daily temperature (in degrees Celsius, °C) and total precipitation (in centimeters) by season and grouped by both level II and level III ecoregions. Data were from Maurer and others (2002).

The biogeochemical modeling framework (chapter 9 of this report) required climate data that characterized the monthly mean of daily minimum and maximum temperatures and the monthly precipitation. For both the model testing period (that is, model spin up) from 1992 to 2000 and the baseline time period (2001–2005), these data were derived from the PRISM climate dataset (Daly and others, 2000; PRISM Climate Group, 2012) at 4-km spatial resolution. The projected monthly mean of daily minimum and maximum temperatures and the projected monthly precipitation were provided by the three GCMs under all three scenarios (Joyce and others, 2011). Change factors were calculated at the original resolution of the GCMs relative to the 1961 to 1990 normals, which were then spatially downscaled using ANUSPLIN software (Hutchinson, 2010) and added to (for temperatures) or multiplied by (for precipitation) the historical normals to produce the future climate projections at 1/12° resolution (approximately 10 km).

7.3. Climate Patterns

Visualizations of seasonal baseline climate patterns and potential future changes are presented in figure 7.3 for each GCM and each climate-change scenario used in the assessment. Descriptions are provided to the extent possible for within-ecoregion variations by using the level III ecoregion names (EPA, 1999); please refer to figure 1.1 of chapter 1 of this report for the geographic locations of the level II and III ecoregions. The seasonal aggregation of results reduced the information about monthly variations while preserving information aligned with the seasonal carbon cycles of winter carbon sources and summer carbon sinks (Miller, 2008). The climate variables included the temperature and precipitation variables used in the disturbance and terrestrial biogeochemical components: mean daily temperature, monthly minimum and maximum temperatures, and total precipitation.

7.3.1. Baseline Climate Patterns of the Western United States

Assessments of climate change are usually made relative to a baseline period that provides benchmark climate summaries. The choice of baseline periods is somewhat arbitrary, but for climate summaries, a 30-year period is desirable. For this general overview of potential long-term climate changes, the baseline period was the recent and relatively stable (climatically) period of 1970 to 1999.

The modeled baseline data indicated that the baseline mean daily temperatures and total precipitation had high spatial and seasonal variability across the Western United States (figs. 7.1 and 7.2). Summer temperatures were most extreme in the Warm Deserts level II ecoregion, where mean daily summer temperatures were as high as 31°C in the Sonoran Basin and Range level III ecoregion. In contrast, the Western Cordillera level II ecoregion tended to include the coldest winter temperatures, with mean daily temperatures reaching as low as −10°C in the Middle Rockies level III ecoregion and −7°C in the Southern Rockies and Wasatch-Uinta Mountains level III ecoregions. The Wyoming Basin level III ecoregion in the Cold Deserts level II ecoregion had the greatest range of seasonal temperatures, with a 24°C difference between summer and winter. In other level II ecoregions, such as the Marine West Coast Forest and Mediterranean California, the seasonal temperature variability was relatively low and temperatures remained above freezing for most of the year.

The Marine West Coast Forest level II ecoregion received extreme precipitation, up to an average of 1,841 millimeters per year (mm/yr). At the other extreme, the annual precipitation in the Warm Deserts and Cold Deserts level II ecoregions averaged only 268 and 313 mm/yr, respectively. For most of the level II ecoregions in the Western United States, the majority of the precipitation fell primarily during the winter, with the spring and fall receiving lesser amounts. Summer tended to be the driest season in most areas except in the Warm Deserts level II ecoregion.

7.3.2. Projected Climate Patterns of the Western United States

The climate projections for 2040 to 2069 were compared with the baseline data from 1960 to 1999 in order to capture gross patterns of climate change. The variability in climate-change projections appeared to be greater among the GCMs than among the three IPCC–SRES scenarios. The maps in figure 7.3 show the projected changes in mean daily temperatures and mean total precipitation, by season, scenario, and GCM. The graphs in figure 7.4 show the projected changes in mean daily temperature and precipitation, by season for each ecoregion. The maps and graphs were based on data from Maurer and others (2007). All of the GCMs projected climate warming throughout the entire region. The projected warming was most pronounced in fall and summer; however, in the northern and central Columbia Plateau and Northern Basin and Range (of the Cold Deserts) and the Blue Mountains and Northern Rockies (of the Western Cordillera), the greater projected increases in mean temperature occurred in the winter and were associated mostly with projected increases in the mean winter minimum temperatures rather than projected increases in the mean winter maximum temperatures. The least amount of projected temperature change occurred in the spring for all ecoregions, with the exceptions of (1) the Warm Deserts and (2) the Arizona-New Mexico Mountains in the southernmost part of the Western Cordillera ecoregion, where the least amount of temperature change occurred in the winter.

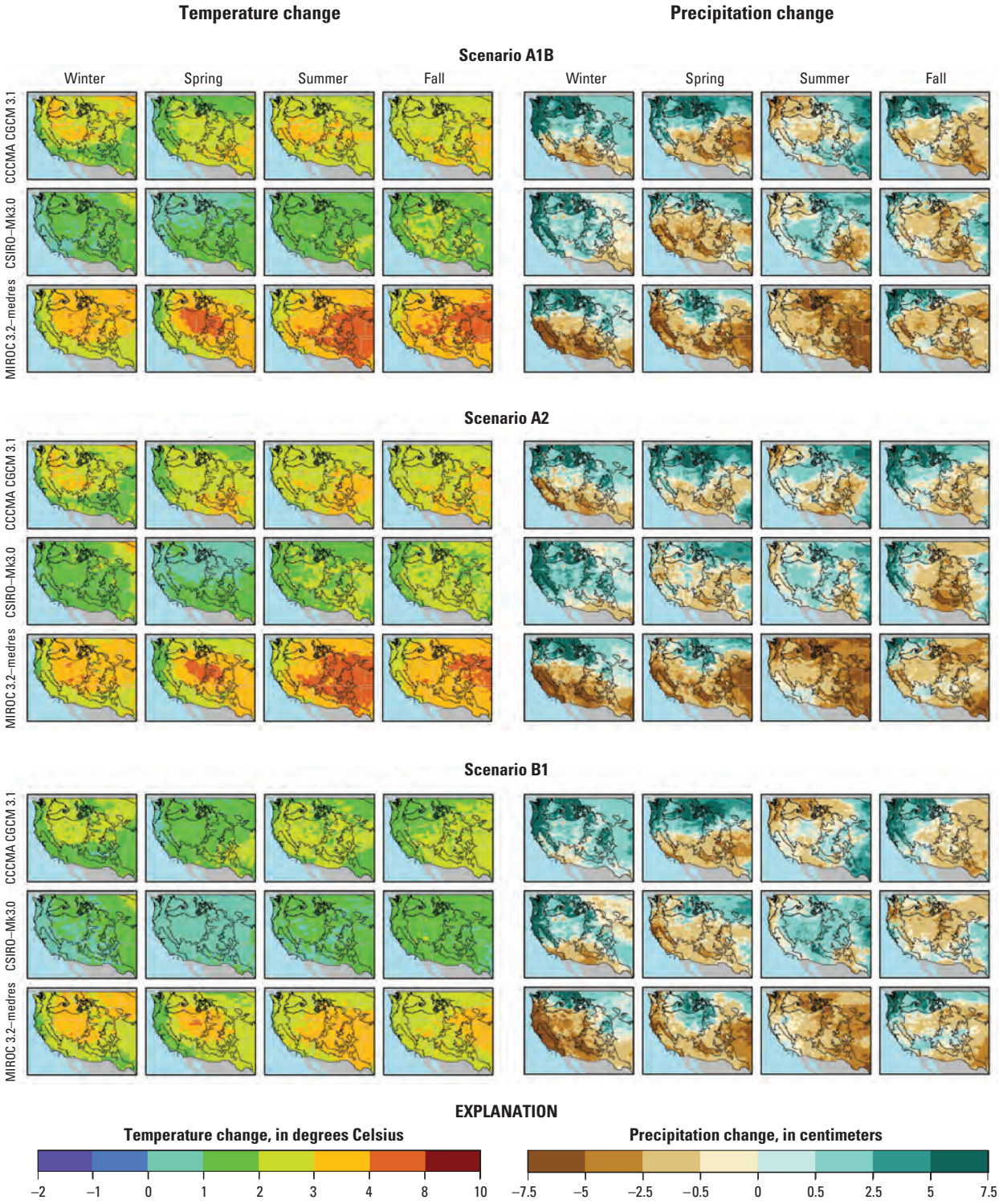

Figure 7.3. Maps showing the projected changes in mean daily temperature (in degrees Celsius, °C) and total precipitation (in centimeters) by season, calculated using the difference in mean values from 2040 to 2069 and from 1970 to 1999. Data were from Maurer and others (2007).

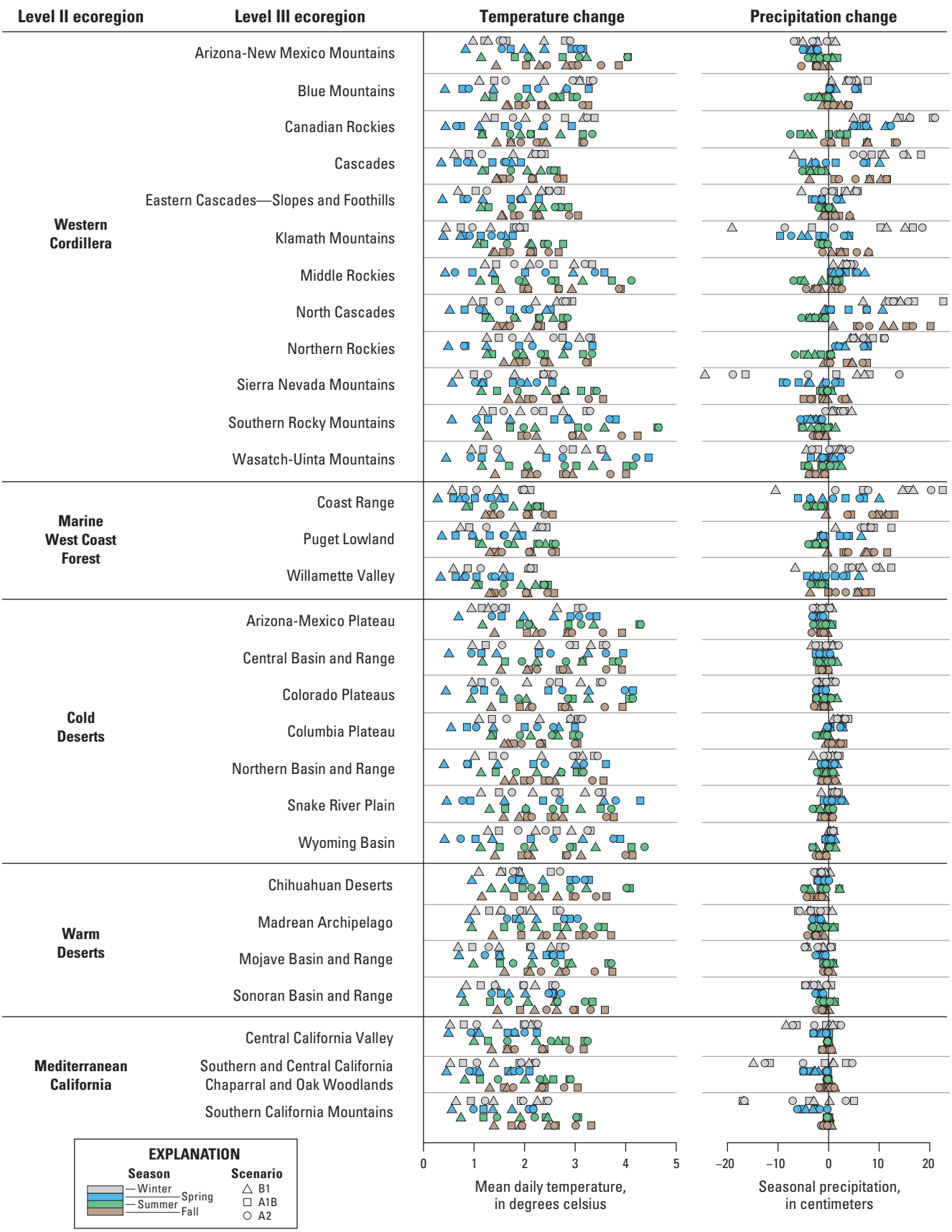

Figure 7.4. Chart showing summaries of the projected seasonal changes in mean daily temperature (in degrees Celsius, °C) and total precipitation (in centimeters) by season and grouped by both level II and III ecoregions for all general circulation models and scenarios. Squares represent the A1B scenario, circles represent the A2 scenario, and triangles represent the B1 scenario. Data were from Maurer and other (2007).

Overall, seasonal warming was projected to be greatest under the A1B and A2 scenarios and least under the B1 scenario. There was variability in the projected temperature changes among the GCMs. The greatest projected increases in mean temperature were from the MIROC 3.2-medres model for the A1B and A2 scenarios in the eastern parts of the Western United States. Specifically, the projected seasonal mean temperature exceeded 4°C during the nonwinter seasons in the Middle Rockies, Wasatch-Uinta Mountains, Southern Rockies, and Arizona-New Mexico Mountains in the eastern Western Cordillera ecoregion; the Wyoming Basin, Colorado Plateaus, and Arizona-New Mexico Plateau in the Cold Deserts ecoregion; and the Chihuahuan Deserts in the Warm Deserts ecoregion. Similarly, the greatest projected increases in mean seasonal maximum temperatures of 4°C to 6°C occurred in these same ecoregions during nonwinter months, particularly in the summer. In contrast, the CSIRO–Mk3.0 model projected the smallest temperature increases. In particular, the projected change in mean spring temperature from the CSIRO–Mk3.0 model for the B1 scenario was less than 0.5°C in the Marine West Coast Forest ecoregion and parts of adjacent regions and in the nearby Eastern Cascades—Slopes and Foothills in the Western Cordillera ecoregion.

Across all of the climate-change scenarios and GCMs, the variability in the projected warming (as measured by the standard deviation) was greatest in the eastern ecoregions of the Western United States and corresponded largely with those ecoregions where relatively large increases in mean and maximum temperatures were projected and least in the western ecoregions located in California and western Oregon and Washington.

The fire-disturbance-modeling data source presented distinct precipitation change patterns in geographical areas of the Western United States. Table 7.1 summarizes these patterns of mean change from all the scenarios and GCMs in terms of level II and level III ecoregions. In this dataset, only the Marine West Coast Forest and Mediterranean California level II ecoregions had a consistent projected seasonal precipitation change pattern across GCMs and scenarios. The projected precipitation patterns varied geographically within the other level II ecoregions. Overall, the projected increases in mean seasonal precipitation occurred in the northern and western portions of the Western United States, especially in the winter, spring, and fall; however, projected summer precipitation tended to decrease in these areas. In the southern and eastern portions of the Western United States, precipitation was projected to decrease during most seasons. In regions where mean seasonal precipitation was projected to decrease, the reductions were most prevalent during the spring and winter (in the west) and during the fall (in the east).

The greatest precipitation reductions were from the MIROC 3.2-medres model. The projected reductions occurred mostly in winter, but also in the spring across all climate-change scenarios in the Mediterranean California ecoregion and in the Sierra Nevada Mountains in the Western Cordillera ecoregion. The projected decreases in mean seasonal precipitation ranged from 7 to 24.5 cm, with the greatest projected decrease occurring in the Sierra Nevada Mountains. Across all of the GCMs, the greater projected precipitation decreases and lesser projected precipitation increases were associated with the B1 scenario. Conversely, the greatest projected seasonal precipitation increases of 10 to 22 cm were associated most often with the A1B and A2 scenarios and by the CCCma CGCM 3.1 model in the winter and fall in the Marine West Coast Forest and in the level III ecoregions within the northern part of the Western Cordillera. The smallest precipitation changes were projected to occur in the central Cold Deserts and in the adjacent Mojave Basin and Range in the Warm Deserts. In relative terms, however, the Warm Deserts and adjacent level III ecoregions were projected to be most affected by proportionate decreases in precipitation across all seasons, scenarios, and GCMs. Decreases in the mean winter and spring precipitation of more than 40 percent were projected by the MIROC 3.2-medres model in these ecoregions. Conversely, the noncoastal ecoregions to the north were projected to receive relatively more precipitation (increases of more than 20 percent in nonsummer months) across all scenarios and GCMs (in particular, the CCCma CGCM3.1 model).

In contrast to the projected mean temperature change, the projected mean seasonal precipitation changes from the two climate data sources diverged in some regions with both negative and positive change. An examination of the terrestrial biogeochemical climate-data source revealed some differences in the climate-change patterns that were mostly explainable in terms of the level II ecoregions. In particular, the mean seasonal precipitation was projected to decrease in all seasons, notably spring and winter, in all of the Western Cordillera level III ecoregions (except for the Arizona-New Mexico Mountains), the Coast Range of the Marine West Coast Forest, and the Northern Basin and Range of the Cold Deserts. Where the projected increases in mean winter precipitation were observed above in table 7.1, projected decreases in winter precipitation prevailed, with the greatest projected decreases in mean winter precipitation occurring in the Canadian Rockies, Sierra Nevada Mountains, and Klamath Mountains, which presented a disagreement with the wildland-fire climate projections of up to 27 cm of mean winter precipitation change. Conversely, for the Southern and Central California Chapparral and Oak Woodlands and the Central California Valley level III ecoregions within the Mediterranean California ecoregion, the reductions in average winter precipitation in the wildland-fire disturbance climate dataset contrasted with increases in average winter precipitation in the terrestrial biogeochemical climate datasets.

Table 7.1. Projected changes in precipitation patterns derived from averaging the results from all the scenarios and general circulation models.

[Data from Maurer and others (2007)]

Projected change in precipitation pattern	Affected level II ecoregions	Affected level III ecoregions
Increases in winter, spring, and fall	Marine West Coast Forest	All.
	Western Cordillera	Cascades, North Cascades, Blue Mountains, Northern Rockies, Canadian Rockies.
	Cold Deserts	Columbia Plateau.
Increases in winter and fall	Western Cordillera	Klamath Mountains, East Cascades—Slope and Foothills.
Increases in winter and spring	Western Cordillera	Middle Rockies.
	Cold Deserts	Wyoming Basin.
Increases in winter	Western Cordillera	Wasatch-Uinta Mountains, Southern Rockies.
	Cold Deserts	Northern Basin and Range.
Decreases in all seasons; greatest decrease in winter and spring	Mediterranean California	All.
	Western Cordillera	Sierra Nevada Mountains.
	Warm Deserts	Mojave Basin and Range, Sonoran Basin and Range.
Decreases in all seasons; greatest decrease in fall and spring	Cold Deserts	Central Basin and Range, Colorado Plateaus, Arizona-New Mexico Plateau.
Decreases in all seasons; greatest decrease in fall, spring, and winter	Western Cordillera	Arizona-New Mexico Mountains.
	Warm Deserts	Madrean Archipelago, Chihuahuan Deserts.

Similarly, the terrestrial biogeochemical climate-change data projected greater precipitation increases, including positive summer precipitation change, in the Puget Lowland and Willamette Valley when using the terrestrial biogeochemical climate-change data compared with the climate-change data related to wildland-fire disturbances. Finally, the terrestrial biogeochemical climate projections indicated less of a decrease in the mean winter precipitation and increases in the mean fall precipitation in the Southern California Mountains and Madrean Archipelago level III ecoregions. Otherwise, mostly in the Warm and Cold Deserts, the projected changes in precipitation patterns in the biochemical climate data were comparable to those described for the wildland-fire-disturbance data.

In addition, proportional seasonal precipitation changes differed between climate data sources. In the biogeochemical model's climate data source, the A2 and A1B scenarios and the MIROC 3.2-medres and CCCma CGCM3.1 models indicated a projected precipitation decrease of approximately 40 percent in the Canadian Rockies during the winter, in the Southern Rockies and Arizona-New Mexico Mountains in the spring, and in the Madrean Archipelago in winter and spring. The B1 and A1B scenarios and mostly the CSIRO–Mk3.0 model indicated a projected seasonal mean precipitation increase of more than 30 percent in the Warm Deserts and Mediterranean California in all seasons except spring, and in the Central Basin and Range and Colorado Plateaus of the Cold Deserts during the summer.

7.4. Summary and Discussion of Caveats Using the Climate Data

Climate data was integral to this assessment and for scenario evaluation. The use of projected future climate-change data, however, contributed to uncertainties in the assessment results. The following caveats should be considered:

- The wildland-fire modeling (chapter 8) and biogeochemical modeling (chapter 9) relied heavily on weather and climate data to characterize baseline conditions and estimate future potential changes, but several different climate and weather datasets were used to complete the simulations. The baseline wildland-fire-disturbance data consistently indicated a wetter baseline climate than did the biogeochemical baseline data; however, the discrepancies that occurred in the projected changes of precipitation patterns, in mountainous areas in particular, were attributable to differences in the downscaled climate projections. In mountainous areas, the interpolation of precipitation patterns have been more challenging because of the orographic effects of the topography (Daly and others, 1993).

- Although future LULC allocation algorithms can incorporate climate-change data to allow for adaptation (Mu and others, 2012), the dynamic interactions between climate and LULC change is currently an unsolved problem (Mendelsohn and Dinar, 2009). For example, the IMAGE 2.2 model was the first to incorporate the consequences of the IPCC–SRES emissions scenarios on the carbon cycle in combination with the dynamically modeled LULC-change maps, but the biogeophysical effects of LULC change were not accounted for in that simple climate model (Sitch, 2005). On the other hand, although the LULC-change scenarios developed for this assessment (chapter 6) did not directly incorporate GCM data, an indirect effect of climate change on the viability and, therefore, resolved demand for future LULC is inherent in the use of the IMAGE 2.2 global model (Image Team, 2001) results. The IMAGE 2.2 model was developed on the basis of an alternative GCM (Hadley Centre Coupled Model 2, HadCM2; Johns and others, 1997). The projected LULC allocations have been further complicated by the projected seasonal changes in precipitation and snowmelt and the implications for irrigation (for example, Vano and others, 2010). This assessment assumes that agricultural irrigation practices were static despite changes in precipitation patterns.

- The assessment of carbon cycling in inland aquatic ecosystems (chapter 10) was for the baseline time period only; projections were not made for future carbon fluxes. The incorporation of climate change into the aquatic system components would require water-discharge projections from downscaled climate predictions and the application of flow-generation models, such as the Precipitation-Runoff Modeling System (PRMS, Leavesley and others, 1983).

- In addition to the documented uncertainties in the GCM outputs, the challenges of using GCMs for modeling effects of climate change in biogeochemical and wildland-fire models included the number of GCM datasets to use in the model runs. In their study of the Western United States, Pierce and others (2009) emphasized the importance of having ensembles of climate model runs with enough realizations to reduce the effects of the natural internal climate variability; they determined that a projected mean derived from a multimodel ensemble was superior to a projected mean derived from just one individual model because of the cancellation of offsetting errors and they advised that five models may be sufficient to derive an appropriate projected mean. There are practical and computational limitations, however, to using multiple GCMs; therefore, only three were used for this assessment.

- The projected potential changes in seasonal temperatures and precipitation were characterized in this chapter to provide a general understanding of when and where climate shifts may occur. Other relevant carbon-cycling models, such as the Palmer Drought Severity Index (PDSI), were not calculated. The wildland-fire projections, however, relied heavily on fuel-moistures data for live and dead biomass, which are a function of temperature, relative humidity, precipitation, and the delayed change in moisture conditions.

This page intentionally left blank.